

# Transmission algorithm for video streaming over cellular networks

Y. Falik · A. Averbuch · U. Yechiali

© Springer Science+Business Media, LLC 2009

**Abstract** 2.5G and 3G cellular networks are becoming more widespread and the need for value added services increases rapidly. One of the key services that operators seek to provide is streaming of rich multimedia content. However, network characteristics make the use of streaming applications very difficult with an unacceptable quality of service (QoS). The 3GPP standardization body has standardized streaming services that will benefit operators and users. There is a need for a mechanism that will enable a good quality multimedia streaming that uses the 3GPP standard. This paper describes an adaptive streaming algorithm that uses the 3GPP standard. It improves significantly the QoS in varying network conditions while monitoring its performance using queueing methodologies. The algorithm utilizes the available buffers on the route of the streaming data in a unique way that guarantees high QoS. The system is analytically modeled: the streaming server, the cellular network and the cellular client are modeled as cascaded buffers and the data is sequentially streamed between them. The proposed Adaptive streaming algorithm (ASA) controls these buffers' occupancy levels by controlling the transmission and the encoding rates of the streaming server to achieve high QoS for the streaming. It overcomes the inherent fluctuations of the network

bandwidth. The algorithm was tested on General Packet Radio Service (GPRS), Enhanced Data rates for GSM Evolution (EDGE) and Universal Mobile Telecommunication System (UMTS) networks. The results showed substantial improvements over other standard streaming methods used today.

**Keywords** Video transmission · Cellular · Modeling, 3GPP · QoS · Adaptive streaming

## 1 Introduction

Streaming video is becoming a common application in 2.5 and 3rd generation cellular networks. The need for value added services in cellular networks is growing rapidly and thus the 3rd Generation Partnership Project (3GPP), which defines the standard for the 3rd generation cellular networks, dedicated a special work group for streaming video [1, 2]. The problem is the low and fluctuated bandwidth of the network that makes a use of streaming applications—while maintaining steady and smooth stream with high (QoS)—very difficult. There are several reasons for bandwidth fluctuations:

*Network load:* In each cell, there is a limited amount of channel resources divided between voice and data sessions. The variation in the number of voice and data sessions and their required resources cause the network to constantly change the channel resources allocated for a streaming session. There is no guarantee for a steady constant bit allocation.

*Radio network conditions:* The radio network conditions may vary during a streaming session because of fading and interference. In order to prevent a packet loss, the

---

Y. Falik · A. Averbuch (✉)  
School of Computer Science, Tel Aviv University,  
Tel Aviv 69978, Israel  
e-mail: amir@math.tau.ac.il  
URL: <http://www.math.tau.ac.il/~amir>

U. Yechiali  
Department of Statistics and Operations Research,  
School of Mathematical Sciences, Tel Aviv University,  
Tel Aviv 69978, Israel

network has a bounded retransmission mechanism, which resends a packet whenever a client fails to receive it. Another mechanism is the forward error correction (FEC) that adds more bits to the data in order to prevent data loss. The FEC level is controlled by the network to match varying network conditions. This results in available bandwidth fluctuation causing congestions and delays.

*Handovers:* Another scenario that causes bandwidth to fluctuate or even momentarily stop is handovers. When a user moves from the coverage area of one network into another, it is called intra-network handovers. When a user moves from the coverage area of a cell to another, the system must provide the capability for that user to remain “in touch” even while breaking the connection with one base station and establishing another connection with another base station. This operation is called inter-network handover.

Another problem that makes streaming in a steady bitrate difficult is finding out the network bandwidth. There is no standard way to acquire bandwidth information from the network. Therefore, we have to rely on reports from the client and it has an unknown delay. The client reports only on an integer number of packets that were received. Usually, to avoid packetization overhead, the size of the packet is very large. Therefore, according to our experience with different telephone type and different cellular network, one packet may be received after up to maximum of 2 s. Thus, the bandwidth can be measured only in large discrete steps with coarse resolution.

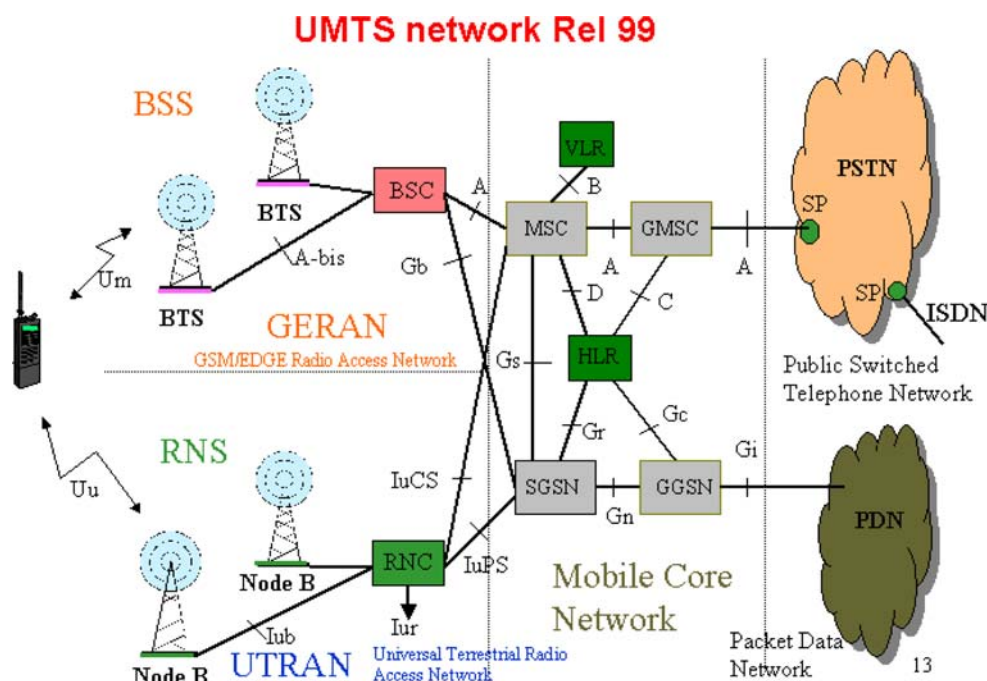
These problems cause the operator to utilize only a fraction of its bandwidth on the one hand, and cause the end user to experience a poor video quality on the other hand.

Figure 1 illustrates the UMTS network architecture. The streaming server resides either in the Internet (PDN in Fig. 1) or usually in the operator premises just before the Gateway GPRS Support Node (GGSN) that acts as a gateway between the UMTS wireless data network and other networks such as the Internet or private networks. The data is passed from the GGSN to the Serving GPRS Support Node (SGSN) that does the full set of interworking with the connected radio network and then to the Radio Network Controller (RNC), which is the governing element in the UMTS radio access network (UTRAN), responsible for control of the base stations (Node-Bs) that are connected to the controller. The RNC carries out radio resource management, some of the mobility management functions and is the point where encryption is done before user’s data is sent to and from the mobile.

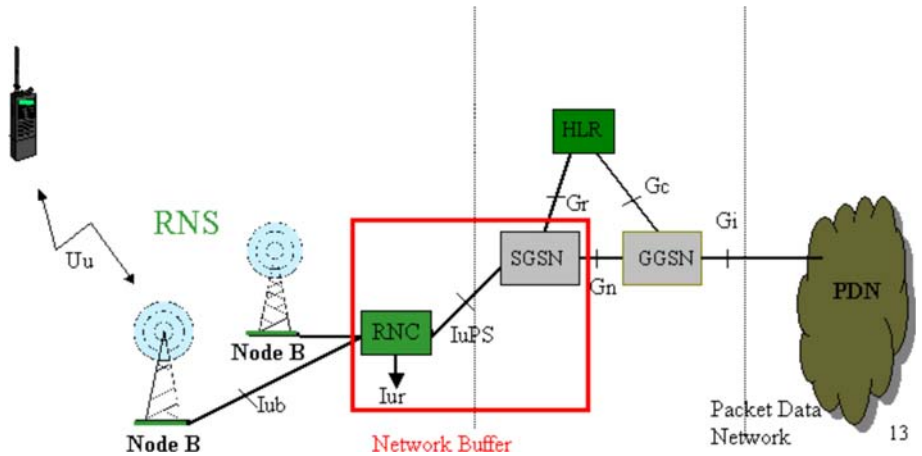
In order to enable handovers between base stations and packet retransmission the data is stored in the buffers of SGSN and RNC (see Fig. 2). These buffers are reallocated for each data session. In this paper, these buffers are considered as a single buffer “The Network buffer”. Although the streaming server does not control the network buffer directly, its behavior during the streaming session is critical in assuring a smooth data stream and a good QoS.

In order to enable a good quality and a smooth multimedia streaming there is a need for adaptive streaming.

**Fig. 1** UMTS architecture.  
 Left: radio access network.  
 Middle: core network. Right:  
 packet-data/telephone network



**Fig. 2** UMTS network buffer—portion of Fig. 1 that is of interest to this paper



The use of constant bit rate media as it comes from the encoder on a varying bit rate channels is not recommended.

The term adaptive here means that a streaming service is able to adapt to varying network conditions. Examples of such variations include variations in throughput, delay and intra/inter-operator roaming to networks with or without QoS support.

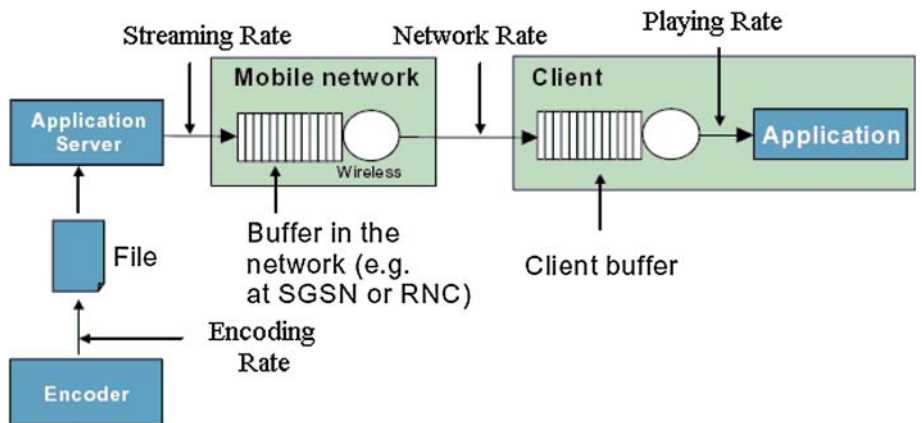
These situations are not very critical for non-real time traffic such as downloading, ftp, browsing. However, they become critical for continuous media transmission, such as streaming, where the user experience drops if the service loses its inherent properties of continuity, synchronization and real-timeness. For instance, continuous (or pause-less) playback is the number one requirement for a successful streaming service. When the network throughput is constantly varying during a session, the effect on the end user’s client is that of a frozen picture, pauses in the audio/video playback, continuous rebufferings (i.e., re-loading from the streaming server a sufficient amount of media data to be streamed with no interruptions) and bad media quality (caused by packet losses caused by network buffers overflow).

Adaptive streaming avoids the above phenomena and ensures pause-less playback to the end user, yielding a

superior user experience compared to conventional streaming. The streaming server uses adaptive streaming by changing the media and the streaming rates. Streaming rate is the rate in which the media is sent from the streaming server to the network. Media rate is the rate in which the media is played (e.g., 32 kbps video means that each second of compressed video is described by 32 kb). The media rate can be changed in live encoding (online) by changing the encoding rate, or in offline by keeping a set of media streams of the same content encoded at different bit rates and performing seamless switch between these different media streams. For example, if a streaming session starts at 64 kbps with good network throughput, and subsequently the network throughput halves, the streaming server can switch to a lower bit rate stream (e.g., 32 kbps) to guarantee pause-less playback and avoid network buffers overflow that can cause packet losses and bad QoS. The server can switch back to the 64 kbps media stream when network conditions improve.

The proposed adaptive media streaming performance is analyzed using methods from queueing theory. For this analysis, the data flow in a streaming session (Fig. 3) is modeled as having one input process (the application server—left of the figure) and two serially connected

**Fig. 3** The modeled multimedia streaming: functional entities



queues—the mobile network buffer (middle of the figure) and the client buffer (right of the figure). The data is delivered from the streaming server to the network, where it is queued (network buffer) and served (transmitted), arriving at the client where it is queued (client jitter buffer) and served (played).

The data flow from the streaming server is controlled. The mobile network buffer queue serves (transmits) the data in a rate that is modeled as a Poisson process [3]. The client queue (Fig. 3) serves (plays) the data in its encoded bit rate. The control mechanism for the streaming server and the performance analysis of the mobile network and the client queues are the subject of this paper.

The physical implementation of the model is illustrated in Fig. 2. The streaming server resides in the PDN, the network buffer is in the SGSN and RNC and the client buffer is in the client.

This paper introduces a model for maintaining a steady QoS for streaming video as described schematically in Fig. 3. An algorithm, which is best-fit for this problem model, is suggested. The algorithm maximizes the streaming session bandwidth utilization while minimizing delays and packet loss. The algorithm can be used on any 3GPP standard client that sends RTCP reports [4]. It was tested on UMTS, EDGE and GPRS networks.

The structure of the paper is as follows. In Sect. 2, we present related work. In Sect. 3, we describe an adaptive streaming algorithm to be used in the streaming server to achieve better QoS. The stochastic performance of the algorithm is described in Sect. 4. Experimental and simulation results on several cellular networks are presented in Sect. 5.

## 2 Related work

### 2.1 Congestion control

In cellular networks, the low and fluctuated bandwidth make streaming applications—while maintaining steady and smooth stream with high QoS—a very difficult task. Congestion control is aimed at solving this problem by adapting the streaming rate to the oscillatory network conditions.

The standardized solution in 3GPP Release 6 to handle adaptive streaming is described in [5, 6]. The 3GPP PSS specifications introduce signaling from the client to the server, which allows the server to have the information it needs in order to best choose both transmission rate and media encoding rate at any time. An adaptive video streaming system, which is compliant with PSS, is described in [7]. This system performs well, but it is different from the proposed algorithm. It does not provide theoretical infrastructure for stream modeling.

The rate adaptation problem is termed curve control [2]. The playout curve shows the cumulative size of the data the decoder has processed by a given time from the client buffer. The encoding curve indicates the progress of data generation if the media encoder runs in real-time. The transmission curve shows the cumulative size of the data sent out by the server at a given time. The reception curve shows the cumulative size of the data received in the client's buffer at a given time.

The distance between the transmission and the reception curves corresponds to the size of the data in the network buffer and the distance between the reception and playout curves corresponds to the size of the data in the client buffer. Curve control here means a limited constrain on the distance between two curves (e.g., by a maximum size of the data, or a maximum delay). This problem is equivalent to controlling the network and the client buffers. However, there is no specific suggestion for choosing the transmission rate and the media encoding rate, and there is no treatment how to handle a client that does not support 3GPP Release 6 signaling.

A widely popular rate control scheme over wired networks is equation-based rate control ([8, 9]), also known as the TCP friendly rate control (TFRC). There are basically three main advantages for a rate control that uses TFRC: first, it does not cause network instability, which means that congestion collapse is avoided. More specifically, TFRC mechanism monitors the status of the network and every time that congestion is detected it adjusts the sending rates of the streaming applications. Second, it is fair for TCP flows, which are the dominant source of traffic on the Internet. Third, the TFRC's rate fluctuation is lower than TCP, thus, making it more appropriate for streaming applications which require constant video quality.

A widely popular model for TFRC is described by

$$T = \frac{kS}{RTT\sqrt{p}}$$

where  $T$  is the sending rate,  $S$  is the packet size,  $RTT$  is the end-to-end round trip time,  $p$  is the end-to-end packet loss rate and  $k$  is a constant factor between 0.7 and 1.3, depending on the particular derivation of the TFRC equation.

The use of TFRC for streaming video over wireless networks is described in [10]. It resolves two TFRC difficulties: first, TFRC assumes that packet loss in wired networks is primarily due to congestion and as such it is not applicable to wireless networks in which the bulk of packet loss is due to error in the physical layer. Second, TFRC does not fully utilize the network channel. It resolves it by multiple TFRC connections that results in full utilization of the network channel. However, it is not possible to use multiple connections in standard 3GPP streaming clients.



The use of TFRC for streaming video over UMTS is given in [11]. The round trip time and the packet loss rate are estimated using the standard real time control protocol (RTCP) RR. The problem of under utilization of one TFRC connection remains.

## 2.2 Video scalability

Adaptive streaming enables to achieve a better QoS compared to conventional streaming. The streaming server uses adaptive streaming by changing the media rate and the streaming rate. Media rate means the bit rate in which the media is encoded/played. The media rate can be changed in live encoding by changing the encoding bit rate or by offline. Several approaches were suggested to enable dynamic bit rate change:

*MPEG-4* ([12]) simple scalable profile is an MPEG-4 tool which enables to change the number of frames per second or the spatial resolution of the media. It encodes the media in several dependent layers and determines the media quality by adding or subtracting layers.

*MPEG-4 Fine granularity scalability (FGS)* is a type of scalability where an enhancement layer can be truncated into any number of bits that provides a corresponding quality enhancement.

A different approach to handle varying encoding bit rates is to use several independent versions of the same media and to switch between these versions. The simplest method is to switch between the versions in key-frames, which are independent frames, that can be decoded independently in any version. Another method, which switches between media versions, creates dedicated P-frames (P-frames are the predicted frames that code the difference between two consecutive frames) that when they are decoded in one version, then contiguous playing from a different version ([13]) is enabled.

H264 SP-frames ([14]) are similar to switching P-frames because they code the difference between frames for different media versions. However, the coding is lossless, therefore, switching between media versions is done without introducing any error to the video stream. The system in [15], which is a variation of [7], presents a streaming system that utilizes interleaved transmission for real-time H264/AVC video in 3G wireless environments without theoretical modeling.

## 3 The Adaptive Streaming Algorithm (ASA)

This section describes the proposed Adaptive Streaming Algorithm (ASA) to be used in the streaming server. A general description of the system is given in Fig. 4. The

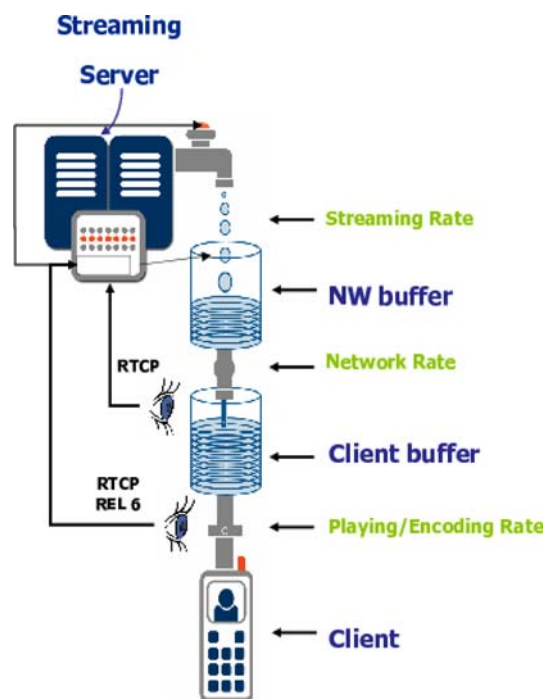


**Fig. 4** Adaptive streaming data and a control flow diagram. The data is passed between the Streaming server, NW and client buffers according to specified rates. The client sends periodic RTCP reports to the Streaming Server enabling to calculate the NW and the client occupancy levels

streaming server controls two transmission parameters: the streaming rate and the encoding rate.

In conventional streaming servers, these two rates are equal to each other, which means that the video clip is streamed at the same rate as it was encoded. The equality of this rate imposes an unnecessary restriction on the system, which causes sub-optimal utilization of the network resources. In the proposed algorithm, this restriction is removed. This enables a full utilization by flexible adaptation to the network resources.

The system is modeled in the following way: the streaming server, the cellular network and the cellular client are modeled as cascaded buffers (see Fig. 4), and the data is passed between them sequentially. The goal of the algorithm is to control all these buffers-occupancy levels by controlling the transmission rate of the streaming server and the decoding rate of the cellular client to achieve streaming with high QoS.

### 3.1 Data flow and buffers

In the ASA model, all the functional entities of the multimedia streaming are considered as buffers (see Fig. 4). Three buffers are used:

*Streaming server buffer:* In an on-demand scenario, the streaming server can use the video file as a buffer and

streams the file faster or slower than the video rate. In a live scenario, the server can delay the video for several seconds and use this data as a buffer. The streaming server controls both the encoding rate of the transmitted media and the data transmission rate. Thus, each transmitted packet has two different size parameters: its size in bits and its duration in media playing time.

*Network buffer:* The network is comprised of several components and network-layers and each component/layer uses a buffer. All these components are connected by a LAN, which is much faster than the rate of a cellular network, thus, all these components can be virtually modeled as a single buffer. The input of this buffer is the output of the streaming server. Its output is the data that is being sent over the mobile network to the client. Its rate is determined by the network conditions and assumed to be a Poisson process. The mobile network buffer has two parameters: its size in bits (occupancy level) and its size in media playing time.

*Client buffer:* The client uses a jitter buffer, which holds the data that is being sent from the network before playing it. Its input is the data received from the network and its output is the media played at the rate it was encoded in. Again, its size can be measured either in bits or in playing time.

### 3.2 Buffer occupancy condition

ASA is designed to assure that during the entire session *each buffer stays in a partially full state—never empty and never full*. This condition will be referred to as the *Buffer Occupancy Condition (BOC)*.

We claim that the BOC enables an optimal utilization of the network resources without degrading the video quality. The reasons are: when the network buffer is empty, the network is idle and wastes potential transmission time. When the network buffer is full, packet loss occurs because the network buffer denies the incoming packets. When the client buffer is empty, the player has to stop the video clip for re-buffering. When the client buffer is full, packet loss occurs, because the client buffer denies the incoming packets.

Conventional streaming servers do not satisfy the BOC condition and usually there are periods that the network is idle.

To apply the BOC, we have to know the bandwidth and occupancy of the mobile network. There is no standard way to query the status of a network and the client buffers. The only available information is the standard RTCP report from the client to the server. In the RTCP report, the client periodically reports to the server the ID of the last packet that was received. This information can be used by the

server to estimate the occupancy of the network buffer and the network data transfer rate. In 3GPP rel. 6, the RTCP receiver reports include also the ID of the last packet that was played in the client. Cellular phones, which comply to 3GPP rel. 6, enable the server to calculate accurately the client buffer occupancy.

In case a cellular phone does not support 3GPP rel. 6, ASA estimates the client buffer occupancy (Sect. 3.3.3).

### 3.3 ASA description

The description of ASA is divided into three sections:

Section 3.3.1 describes the way ASA controls the network buffer occupancy level by changing the streaming rate.

Section 3.3.2 describes the way ASA controls the client buffer occupancy level by changing the encoding rate and by controlling the network buffer occupancy level. The control is based on 3GPP Rel. 6 information.

Section 3.3.3 describes the way ASA controls the client buffer occupancy level based on the occupancy estimation when 3GPP Rel. 6 information is unavailable.

Notation:

$R_{NW}(t)$	The cellular network outgoing rate at instant $t$ .
$R_S(t)$	The streaming server outgoing rate at instant $t$ .
$R_S^E(t)$	The streaming server encoding rate at instant $t$ . It is also the client playback rate after an unknown delay, because the streamed packets are eventually played by the client at the encoding rate.
$O_{NW}(t)$	The occupancy level of the network buffer in bits at instant $t$ .
$D_{NW}(t)$	The duration of playing time in the network buffer at instant $t$ .
$DO_{NW}$	The desired occupancy level of the network buffer in bits.
$T_{ADJ}$	An adjustment period.
$D_C(t)$	The duration of playing time in the client buffer at instant $t$ .
$D_C^D$	The desired duration of playing time in the client buffer.
$P_S^{SE}(t)$	The ratio between the streaming and encoding rate at instant $t$ .
$D_S(t)$	The duration of playing time in the streaming server buffer at instant $t$ . $D_S(t) \neq 0$ when the streaming and the encoding rates differ.

#### 3.3.1 Network buffer

In order to satisfy the BOC, we first try to maintain the network buffer filled with as little data as possible without ever being actually empty. We wish to achieve a

constant occupancy level. The occupancy level  $O_{NW}(t)$  is affected by the network input and output rates. The output rate  $R_{NW}(t)$  is the network data output rate, which is not controlled by our application. The input rate  $R_S(t)$  is the streaming server rate, which is fully controllable. It is important to note that the video encoding rate  $R_S^E(t)$  does not affect the network buffer occupancy level, because the rate in which data enters the network buffer is determined by the streaming server outgoing rate  $R_S(t)$ . The video encoding rate  $R_S^E(t)$  determines the playback rate of the video which affects the client and not the network.

The flow of ASA is given in Fig. 5. The calculation of the streaming rate  $R_S(t)$  at time  $t$  (“streaming rate calculation” in Fig. 5) takes into account the previous network rate  $R_{NW}(t - \tau)$  in  $\tau$  units of time before, as a prediction for the next network rate  $R_{NW}(t)$ . It adds to it a factor that should adjust the occupancy level  $O_{NW}(t)$  to some predetermined desired occupancy level  $DO_{NW}$  after some predetermined adjustment period  $T_{ADJ}$ . More formally, the streaming rate is determined by:

$$R_S(t) = R_{NW}(t - \tau) + \frac{DO_{NW} - O_{NW}(t - \tau)}{T_{ADJ}} \cdot \tau, \quad (1)$$

$$0 \leq \tau \leq T_{ADJ}.$$

$R_S(t)$  is computed every time an RTCP Receiver Report (RTCP RR) is received by the streaming server.  $\tau$  is the time difference between two RTCP RRs.

$R_{NW}(t - \tau)$  and  $O_{NW}(t - \tau)$  are calculated using information from the RTCP RR. Every RTCP RR packet contains the ID of the last UDP packet that was received by the client and also the time the RTCP RR was sent. The streaming server should create a table of all the sent UDP packets, their ID's, sent times and sizes.  $R_{NW}(t - \tau)$  is the total size of the UDP packets that were received by the client between the last two RTCP RRs, divided by the RTCP RRs' time difference.  $O_{NW}(t - \tau)$  is the total size of the UDP packets that were in the NW buffer at time  $t - \tau$ . The last packet in the NW buffer is the UDP packet that was sent by the streaming server at time  $t - \tau$ , this packet is found in the UDP table. The first packet in the NW buffer is the packet preceding the UDP packet that was received by the client at that time. It is reported in the RTCP RR and found in the UDP table. The total size of the UDP packets between these two packets is calculated using the UDP table. The desired network occupancy level  $DO_{NW}$  and the adjustment-period  $T_{ADJ}$  are parameters of the algorithm that differ for different network types such as GPRS and UMTS. Their actual values are empirically tuned. For example,  $DO_{NW}$  can be the expected average number of bits to be streamed in half a second and  $T_{ADJ}$  can be one second.

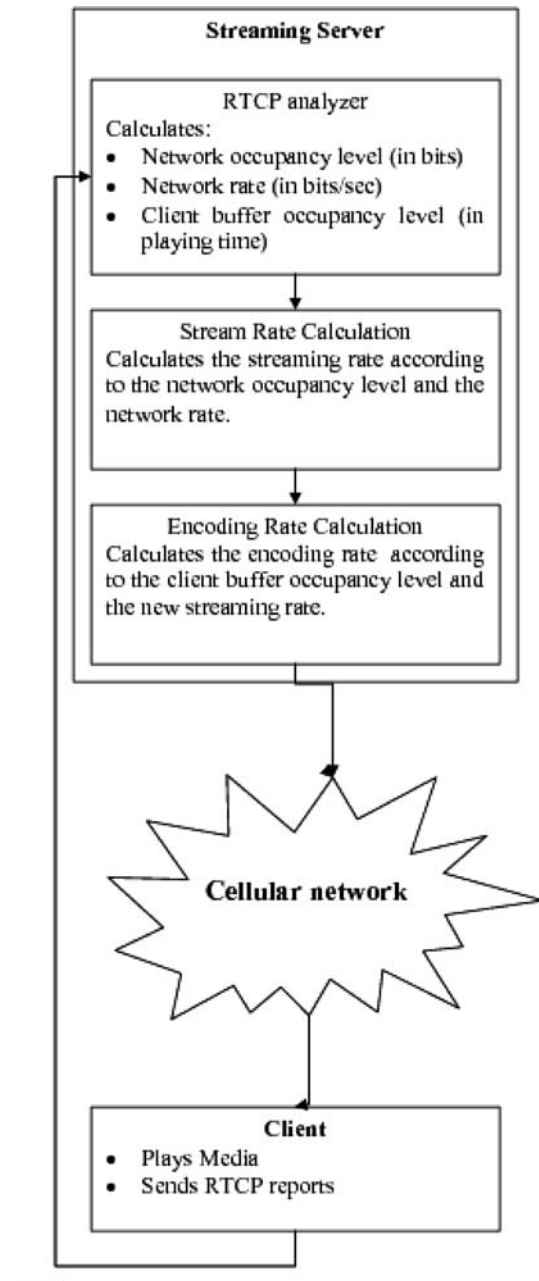


Fig. 5 ASA flow

The network rate  $R_{NW}(t)$  and the network buffer occupancy level  $O_{NW}(t)$  are measured through reports from the client. We rely on the standard RTCP receiver report that every 3GPP standard client sends. The server calculates from each RTCP receiver report these parameters and prescribes the streaming-rate  $R_S(t)$  accordingly. This streaming-rate should adaptively keep the network-buffer occupancy  $O_{NW}(t)$  close to the desired occupancy level  $DO_{NW}$ .

*Example:* Assume the streaming session begins with a streaming rate of 10 kbps while the potential network rate

is a constant 30 kbps. The streaming server cannot know the potential network rate, but since the network buffer will be empty after the first RTCP report, it raises the streaming rate. Then, data will start to accumulate in the network buffer. Subsequently, the network buffer reaches its desired occupancy level and then the streaming rate will decrease until it will equate the network rate. Then, the network buffer will remain at the constant desired occupancy level.

Throughout the session, a change in the network potential rate will only appear in the actual network rate when the network buffer is neither empty nor full.

If the network rate increases, the occupancy level of the buffer decreases, and, thus, the streaming rate will increase as a compensation until again the buffer will reach its desired occupancy level and the two rates will equate.

Similarly, if the network rate decreases, the occupancy level of its buffer-occupancy increases, and, thus, the streaming rate decreases as a compensation until again the buffer will reach its desired occupancy level and the two rates will equate.

### 3.3.2 Client buffer

The occupancy level of the client buffer is influenced by its input and output rates. The input rate  $R_{NW}(t)$  is the network transmission rate, which we have no control over. The output rate  $R_S^E(t)$  is the encoding rate, which is controllable. Therefore, in order to maintain the client buffer in a partially-full state (satisfying BOC), we have to control the encoding rate.

The method that determines the encoding rate (“Encoding rate calculation” in Fig. 5) is similar to the method used to determine the streaming rate, except that instead of using buffer size in bits, we use the buffer size in playing time. The occupancy level of the client buffer in playing time is influenced by the outgoing playing time rate which is 1 because in each second one second of video is played by the client, and the incoming playing time rate, which is the network rate divided by the encoding rate of the packets that enter the client. We cannot control the packets that enter the client directly so instead we control the packets that are streamed and will enter the client after a short delay. The streamed packets playing time rate is the streaming rate divided by the encoding rate. Again, we set a desired occupancy level (in playing time) and an adjustment-period and if we assume that the network rate will stay the same and want to reach the desired client occupancy level in  $T_{ADJ}$  time then:

$$\frac{R_S(t)}{R_S^E(t)} - 1 = \frac{D_C^D - D_C(t)}{T_{ADJ}}.$$

and:

$$P_S^{SE}(t) = \frac{R_S(t)}{R_S^E(t)} = 1 + \frac{D_C^D - D_C(t)}{T_{ADJ}}.$$

$P_S^{SE}(t)$  is computed each time an RTCP receiver report is received in the streaming server.

The client plays the media at the same rate at which it is encoded, which accounts for the ‘1’ in the formula.

The actual encoding rate is

$$R_S^E(t) = \frac{R_S(t)}{P_S^{SE}(t)}.$$

The control over the network buffer is direct. Any change in the streaming rate directly affects the occupancy level. It differs from the control over the client buffer which is delayed. The media data has to pass through the network buffer first. This delay might be crucial when the network available bandwidth drastically decreases. In order to avoid this problem, we try to maintain the network buffer filled with as little data as possible without ever being actually empty.

The separation between the streaming and encoding rates is more important in the case of scalable video. In this case, only a limited number of encoding rates are available. When scalable video is used, ASA will choose the video level with an encoding rate just below the calculated encoding rate. The separation between the rates enables a smooth transmission and a better utilization of the network although we have a limited number of encoding rates. For example, assume the average of the network rate  $R_{NW}(t)$  is 50 kbps with jitter around the average. The encoding rate  $R_S^E(t)$  will remain 50 kbps. However, the streaming rate  $R_S(t)$  will follow the jittering network rate. In case the network rate drops, the streaming rate will drop quickly afterwards to prevent network buffer overflow. Then, the streaming rate will follow.

A real time transcoder with no internal buffer will be unable to separate between streaming and encoding rates. Therefore, first the streaming rate  $R_S(t)$  and then the encoding rate  $R_S^E(t)$  are calculated. The mutual streaming/encoding rate will be  $R_S(t) = R_S^E(t) = \text{Min}(R_S(t), R_S^E(t))$ . Thus, network buffer overflow and client buffer underflow are prevented.

### 3.3.3 Client buffer occupancy estimation

The client buffer occupancy level is reported in 3GPP rel. 6. The majority of the clients do not support rel. 6 and the client buffer occupancy level is unknown. Therefore, we estimate its occupancy.

This estimate is based on the duration of playing time in each streaming server, network and client buffers. The sum



of playing time at the three buffers is  $D_S(t) + D_{NW}(t) + D_C(t) = \text{constant}$  during the streaming session (this is true as long as the client did not stop for re-buffering). The above sum of playing time is constant because the media enters the streaming server at the encoding rate leaves the client buffer at the same encoding rate, as long as both do not stop playing. The sum of playing time is simply the time difference between the moment the streaming server starts streaming and the moment the client starts playing.

The duration of playing time in the streaming server buffer  $D_S(t)$  is the difference between the playing time and the transmission time of the last sent packet. The duration of playing time in the network buffer  $D_{NW}(t)$  is the difference between the playing time stamps of the last sent packet and the last received packet sent by the client RTCP report.

The duration of playing time in the client buffer  $D_C(t)$  is not known but can be calculated directly from the duration of playing time in the streaming server and the network buffer which is known. Therefore,

$$D_C(t) = \text{constant} - D_S(t) - D_{NW}(t). \tag{2}$$

The constant in Eq. 2 is not known but its value is not so important because we only need to monitor the change in the duration of playing time in the client buffer  $D_C(t)$  and not its absolute value.

#### 4 Stochastic analysis of ASA performance

In this section, we present a stochastic analysis of the performance of ASA. We focus on the mobile network buffer occupancy control regardless of whether or not the client sends 3GPP Rel. 6 reports. The client buffer occupancy level is the complement of the network buffer occupancy level measured in playing time.

Let  $R_{NW}(t)$  be a Poisson random variable, with intensity  $\lambda$ , describing the number of bits transmitted by the network during the time interval  $(t - \tau, t]$ ,  $t > \tau > 0$ . That is:

$$P\{R_{NW}(t) = n\} = e^{-\lambda\tau} \frac{(\lambda\tau)^n}{n!}, \quad t, \tau \in \mathbb{R}^+, n \in \mathbb{N}. \tag{3}$$

For any  $t > 0$ , the number of bits  $R_S(t)$  transmitted to the network in time interval  $(t - \tau, t]$  (see Fig. 6) is determined by the streaming server as in Eq. 1 where, as indicated,  $O_{NW}(t)$  and  $DO_{NW}$  (see Fig. 6) are the occupancy level of the mobile network buffer at instant  $t$  and the desired occupancy level, respectively.  $T_{ADJ}$  is a time constant.  $R_{NW}(t - \tau)$  in Eq. 1 approximates  $R_{NW}(t)$ , while  $\frac{DO_{NW} - O_{NW}(t - \tau)}{T_{ADJ}} \cdot \tau$  is a correction element that aims at bringing the network buffer occupancy level  $O_{NW}(t)$  to the desired occupancy level  $DO_{NW}$  after a period  $T_{ADJ}$ . For

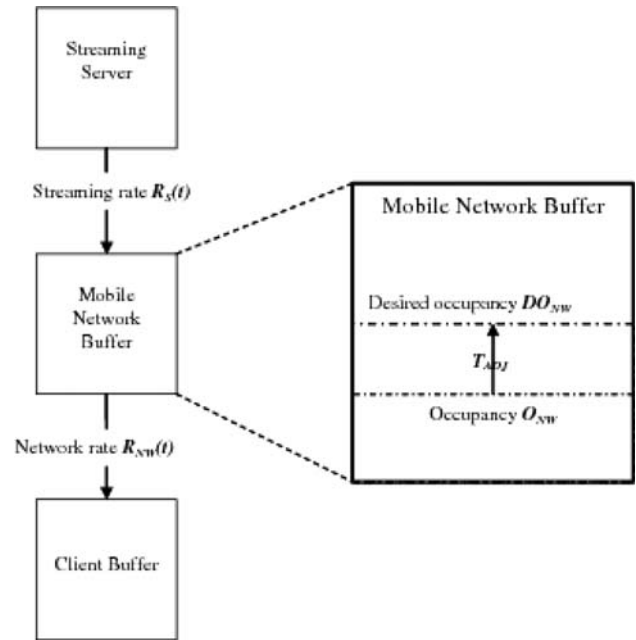


Fig. 6 ASA parameters

example, assume that the desired occupancy level  $DO_{NW}$  is 80,000 bits and from the last RTCP receiver report (RR) we calculate that the network transmitted  $R_{NW}(t - \tau) = 50,000$  bits and the network occupancy level  $O_{NW}(t)$  is 60,000 bits. We also know that the RTCP RR interval is  $\tau = 1$  s. In response, the streaming server adjusts the streaming rate  $R_S(t)$  to be  $R_S(t) = 50,000 + \frac{80,000 - 60,000}{2} \cdot 1 = 60,000$  bits, which is higher than the network rate. Therefore, the occupancy level  $O_{NW}(t)$  becomes close to the desired occupancy level  $DO_{NW}$ .

##### 4.1 Analysis of ASA performance using Gaussian approximation

We assume that  $R_{NW}(t - \tau)$  in Eq. 1 is independent of  $O_{NW}(t - \tau)$ . While this is not accurate, it fits the spirit of the algorithm, as we are not using  $R_{NW}(t - \tau)$  because of its value in the previous time step, but as an approximation to  $R_{NW}(t)$  in the current time step.

To simplify the computations, we assume that the occupancy of the network buffer can be negative.

The mobile network buffer can be analyzed as a Markov process  $O_{NW}(t)$ :  $O_{NW}(t) = i$  when the network buffer is filled with  $i$  bits. The stationary distribution  $P_i$  is the probability that the process has value  $i$  in steady state. The transition probability  $P_{ij}$  is the probability for the transition from  $O_{NW}(t - \tau) = i$  to  $O_{NW}(t) = j$ . Formally,

$$P_{ij} = P\{O_{NW}(t) = j \mid O_{NW}(t - \tau) = i\}. \tag{4}$$

The occupancy level is the previous occupancy level plus the difference in the incoming and outgoing data rates, i.e.

$$O_{NW}(t) = O_{NW}(t - \tau) + R_S(t) - R_{NW}(t). \tag{5}$$

Substituting Eq. 1 in Eq. 5 and get

$$O_{NW}(t) \sim O_{NW}(t - \tau) + \frac{DO_{NW} - O_{NW}(t - \tau)}{T_{ADJ}}\tau + R_{NW}(t - \tau) - R_{NW}(t). \tag{6}$$

By replacing the rates difference in Eq. 6 with the Skellam distribution (see below) and using  $T_R \triangleq \frac{T_{ADJ}}{\tau}$ , we get

$$O_{NW}(t) \sim \text{skellam}(\lambda\tau) + \frac{DO_{NW}}{T_R} + \frac{T_R - 1}{T_R}O_{NW}(t - \tau). \tag{7}$$

When in stationary state,  $O_{NW}(t)$  and  $O_{NW}(t - \tau)$  are identically distributed having the same mean  $E\{O_{NW}(t)\} = E\{O_{NW}(t - \tau)\} = \mu$  and the same variance  $\text{var}\{O_{NW}(t)\} = \text{var}\{O_{NW}(t - \tau)\} = \sigma^2$ . Also, the Skellam's mean is 0 and its variance equals  $2\lambda\tau$ . By taking expectation of both sides of Eq. 7, we get

$$E\{O_{NW}(t)\} = E\{\text{skellam}(\lambda\tau) + \frac{DO_{NW}}{T_R} + \frac{T_R - 1}{T_R}O_{NW}(t - \tau)\}. \tag{8}$$

Using stationarity and substituting  $E\{O_{NW}(t)\} = \mu$  yields

$$\mu = 0 + \frac{DO_{NW}}{T_R} + \frac{T_R - 1}{T_R}\mu. \tag{9}$$

This implies that  $\mu = DO_{NW}$ .

In the same way, we calculate the variance of  $O_{NW}(t)$  according to Eq. 7 and get

$$\text{var}\{O_{NW}(t)\} = \text{var}\{\text{skellam}(\lambda\tau) + \frac{DO_{NW}}{T_R} + \frac{T_R - 1}{T_R}O_{NW}(t - \tau)\}. \tag{10}$$

Substituting  $\text{var}\{O_{NW}(t)\} = \sigma^2$  and assuming all RVs in Eq. 10 to be independent, we have

$$\sigma^2 = 2\lambda\tau + 0 + \left(\frac{T_R - 1}{T_R}\right)^2 \sigma^2. \tag{11}$$

From Eq. 11 we get  $\sigma^2 = \frac{2\lambda\tau T_R^2}{2T_R - 1}$ .

Actually, this result applies to any outgoing bit rate distribution. As long as it is memory-less and its variance  $\sigma_{NW}^2$  is known, we have

$$\sigma^2 = \frac{2\sigma_{NW}^2 T_R^2}{2T_R - 1}, \quad \mu = DO_{NW}.$$

Substituting Eq. 5 in Eq. 4 and get

$$P_{i,j} = P\{O_{NW}(t - \tau) + [R_S(t) - R_{NW}(t)] = j \mid O_{NW}(t - \tau) = i\}. \tag{12}$$

Substituting Eq. 1 in Eq. 12 (while denoting  $T_R \triangleq \frac{T_{ADJ}}{\tau}$ ) leads to

$$\begin{aligned} P_{i,j} &= P\left\{O_{NW}(t - \tau) + \left[\frac{DO_{NW} - O_{NW}(t - \tau)}{T_R} + R_{NW}(t - \tau) - R_{NW}(t)\right] = j \mid O_{NW}(t - \tau) = i\right\} \\ &= P\left\{i + \left[\frac{DO_{NW} - i}{T_R} + R_{NW}(t - \tau) - R_{NW}(t)\right] = j \mid O_{NW}(t - \tau) = i\right\}. \end{aligned}$$

Subtracting  $i + \frac{DO_{NW} - i}{T_R}$  from both sides results in

$$\begin{aligned} P_{i,j} &= P\left\{[R_{NW}(t - \tau) - R_{NW}(t)] = j - i - \frac{DO_{NW} - i}{T_R} \mid O_{NW}(t - \tau) = i\right\}. \end{aligned}$$

Since both  $R_{NW}(t)$  and  $R_{NW}(t - \tau)$  are independent of  $O_{NW}(t - \tau)$  we get

$$P_{i,j} = P\left\{[R_{NW}(t - \tau) - R_{NW}(t)] = j - i - \frac{DO_{NW} - i}{T_R}\right\}. \tag{13}$$

In order to solve Eq. 13, we have to find the distribution of  $R_{NW}(t - \tau) - R_{NW}(t)$ . Assuming that the network rate  $R_{NW}(t)$  and its occupancy  $O_{NW}(t)$  are independent,  $R_{NW}(t - \tau) - R_{NW}(t)$  is the difference between two i.i.d Poisson random variables with intensity  $\lambda$ . This difference, as noted, is called Skellam distribution [16], and can be approximated as Gaussian with expectation 0 and variance  $2\lambda\tau$ . Since Gaussian is a continuous distribution, we analyze the occupancy as a continuous variable. From now on, we denote by  $f(i)$  the density function of  $O_{NW}(t)$  and by  $f(i, j)$  the density function of the transition probability of  $O_{NW}(t - \tau)$  to  $O_{NW}(t)$ .

Denote by  $\gamma_{\mu, \sigma^2}$  the density function of the Gaussian distribution  $\gamma_{\mu, \sigma^2}(x) = \frac{1}{\sigma\sqrt{2\pi}}e^{-\frac{(x-\mu)^2}{2\sigma^2}}$ , then

$$f(i, j) = \gamma_{0, 2\lambda\tau}\left(j - i - \frac{DO_{NW} - i}{T_R}\right) = \frac{1}{\sqrt{4\pi\lambda\tau}}e^{-\frac{(j-i-\frac{DO_{NW}-i}{T_R})^2}{4\lambda\tau}}. \tag{14}$$

For the Markov chain, the stationary distribution and the transition probabilities satisfy the balance equation

$$P_j = \sum_{i=0}^{\infty} P_i \cdot P_{i,j}, \quad \sum_{i=0}^{\infty} P_i = 1. \tag{15}$$

For approximating continuous process, we write

$$f(j) = \int_{-\infty}^{\infty} f(i) \cdot f(i, j) di \tag{16}$$

where  $di$  replaces the common representation  $dx$ . We now substitute Eq. 14 in Eq. 16 and get

$$f(j) = \int_{-\infty}^{\infty} \left[ f(i) \cdot \frac{1}{\sqrt{4\pi\lambda\tau}} \cdot e^{-\frac{(j-i-\frac{DO_{NW}-i}{T_R})^2}{4\lambda\tau}} \right] di. \tag{17}$$

The uniqueness of  $P_i$ 's implies that if we validate that a certain stationary distribution satisfies the balance equation (Eq. 15), then this is the only solution. We now show that the stationary distribution  $f(i)$  is a Gaussian distribution with  $\sigma^2 = \frac{2\lambda\tau T_R^2}{2T_R-1}$ th mean  $\mu = DO_{NW}$  and variance. Thus, in Eq. 17, we substitute  $f(j) = \alpha DO_{NW, \sigma^2}(j)$  and  $f(i) = \alpha DO_{NW, \sigma^2}(i)$  to get

$$\begin{aligned} & \frac{1}{\sqrt{2\pi} \cdot \sigma} \cdot e^{-\frac{(j-DO_{NW})^2}{2\sigma^2}} \\ &= \int_{-\infty}^{\infty} \left[ \frac{1}{\sqrt{2\pi} \cdot \sigma} \cdot e^{-\frac{(i-DO_{NW})^2}{2\sigma^2}} \cdot \frac{1}{\sqrt{4\pi\lambda\tau}} \cdot e^{-\frac{(j-i-\frac{DO_{NW}-i}{T_R})^2}{4\lambda\tau}} \right] di. \end{aligned} \tag{18}$$

Dividing Eq. 18 by  $f(j)$  we get:

$$1 = \int_{-\infty}^{\infty} \left[ \frac{1}{\sqrt{4\pi\lambda\tau}} \cdot e^{-\left[ \frac{-(i-DO_{NW})^2}{2\sigma^2} + \frac{-(j-i-\frac{DO_{NW}-i}{T_R})^2}{4\lambda\tau} - \frac{-(j-DO_{NW})^2}{2\sigma^2} \right]} \right] di. \tag{19}$$

Setting  $\sigma^2 \triangleq \frac{2\lambda\tau T_R^2}{2T_R-1}$  in the integrand in Eq. 19 leads to

$$\begin{aligned} & \frac{1}{\sqrt{4\pi\lambda\tau}} \cdot e^{-\left[ \frac{-(i-DO_{NW})^2}{\frac{4\lambda\tau T_R^2}{2T_R-1}} + \frac{-(j-i-\frac{DO_{NW}-i}{T_R})^2}{4\lambda\tau} - \frac{-(j-DO_{NW})^2}{\frac{4\lambda\tau T_R^2}{2T_R-1}} \right]} \\ &= \frac{1}{\sqrt{4\pi\lambda\tau}} \cdot e^{-\frac{\left( i - \left( DO_{NW} + \frac{(jT_R - DO_{NW})(T_R - 1)}{T_R^2} \right) \right)^2}{4\lambda\tau}}. \end{aligned}$$

That is, the integrand in Eq. 19 is the normal distribution with density  $\gamma_{\mu, 2\lambda\tau}(i)$ , where  $\mu = DO_{NW} + \frac{(jT_R - DO_{NW})(T_R - 1)}{T_R^2}$ .

Thus, we proved that the stationary distribution  $f(i)$  is a Gaussian,  $f(i) \approx N\left(DO_{NW}, \frac{2\lambda\tau T_R^2}{2T_R-1}\right)$ . The stationary density  $f(i)$  is calculated for GPRS networking in Fig. 7.

We conclude:

- The occupancy of the network buffer can be approximated by a normal distribution around  $DO_{NW}$ .
- $T_R$  is the ratio between the time  $T_{ADJ}$  it takes for the streaming server to correct the occupancy and the sampling time  $\tau$ . We are interested in values of  $T_R$  that are greater than 1. For these values, when  $T_R$  grows, the variance grows as well.
- When  $T_R = \frac{1}{2}$ , the variance is infinite. It means that if the streaming server reacts too fast. The system will constantly oscillate without reaching stationarity.

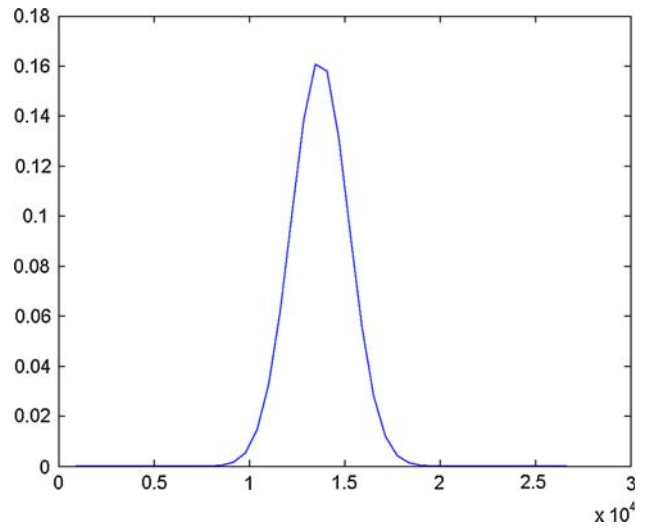


**Fig. 7** Network buffer occupancy  $O_{NW}(t)$  density function for GPRS. The  $x$ -axis is the occupancy level of the network buffer in bits. We assume that the RTP packet size is 500 bytes, the desired occupancy level  $DO_{NW}$  is 14,000 bytes, the average network rate  $\lambda$  is 15,000 kbps and  $T_R = 1$

- By differentiating the variance  $\sigma^2 = \frac{2\lambda\tau T_R^2}{2T_R-1}$  with respect to  $T_R$  we get  $\frac{\partial \sigma^2}{\partial T_R} = \frac{4\lambda\tau T_R(T_R-1)}{(2T_R-1)^2}$ , and we see that the variance is minimal when  $T_R = 1$ .

## 5 Experimental and simulation results

### 5.1 Experimental results

The ASA was implemented on several commercial cellular networks. The architecture is comprised of a streaming server, a real time transcoder and a cellular client (see Fig. 8). The streaming server is located in the Internet and the transcoder is located between the streaming server and the cellular client. The streaming server and the real time transcoder used RTP/RTSP [17] protocols to stream the media.

The real time transcoder transcodes the incoming media to a format and parameters that are supported by the cellular client. It uses ASA to adapt the transcoded media to the network conditions. In our case, the transcoded media is 3GP file format, MPEG-4 simple profile video codec that operates on QCIF (176 × 144) with 3–30 frames per second. This architecture is close to the one given in Fig. 3 except that here the content resides in the Internet where in Fig. 3 it resides in the streaming server.

The results are given from live UMTS, EDGE and GPRS networks. The  $x$ -axis in Figs. 9, 10, 11, 12—presents the RTCP RR number. The average RTCP RR interval is approximately 900 ms.

Figure 9 depicts the UMTS network rate as calculated from the client RTCP RR. The network rate the ASA

**Fig. 8** The architecture for the experimental setup: A real time transcoder using ASA is located between the streaming server and the cellular client

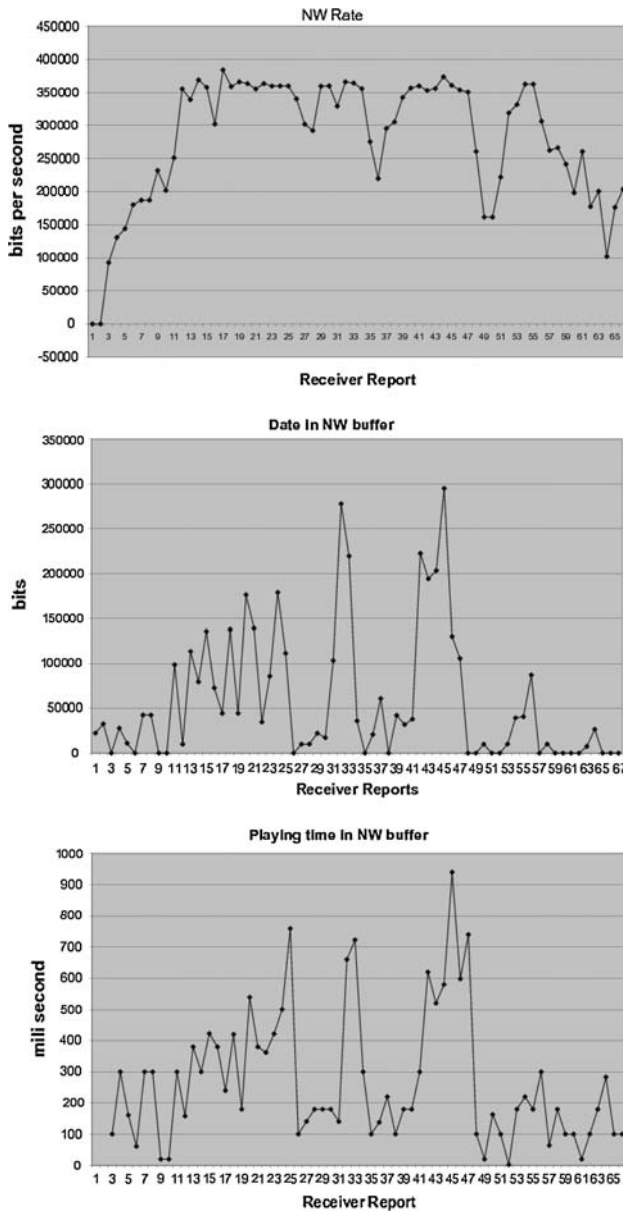
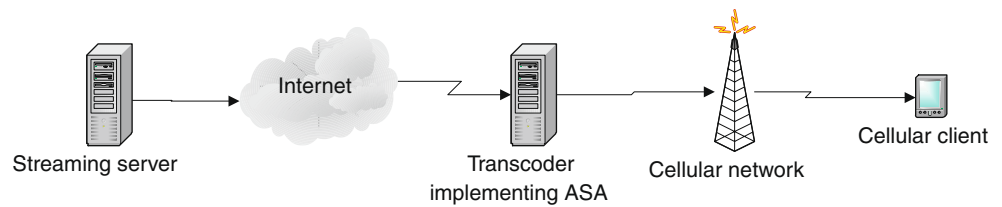


**Fig. 9** Top: Network rate  $R_{NW}(t)$ . Middle: Data level  $O_{NW}(t)$ . Bottom: playing-time  $D_{NW}(t)$ . All calculations are based on RTCP RR for UMTS

achieved is very high: we can see long periods of 360 kbps (top) which is near the maximal 384 kbps UMTS rate. The starting rate is configured to be 90 kbps but the transcoder quickly increases it because the network buffer is empty.

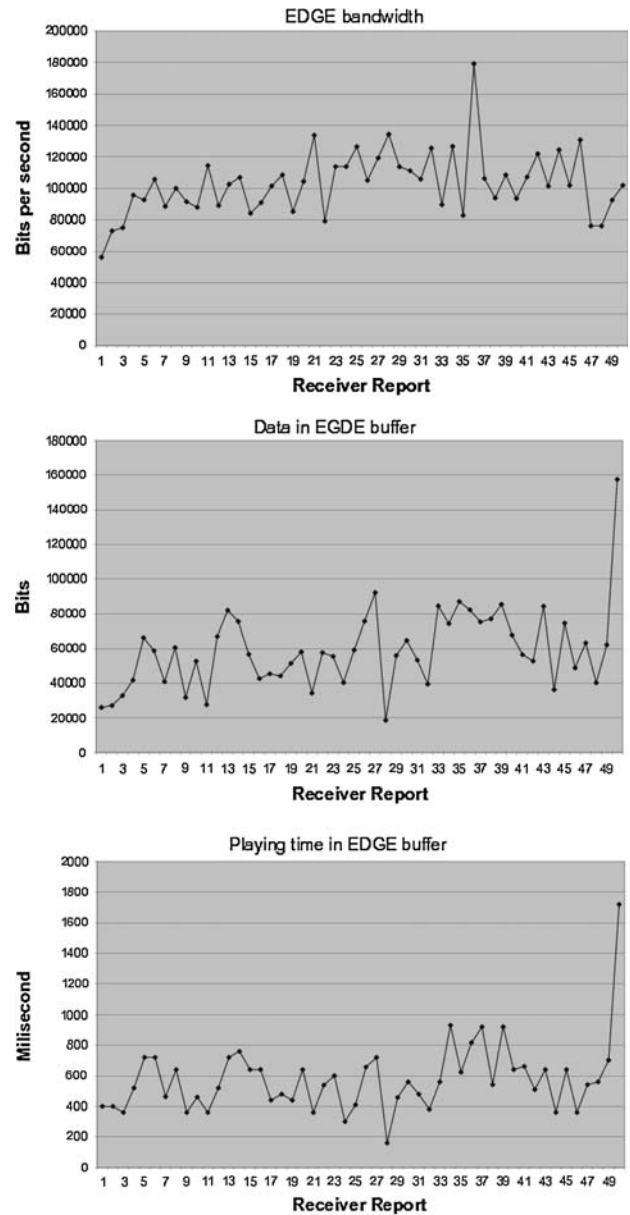


**Fig. 10** Top: Network rate  $R_{NW}(t)$ . Middle: Data level  $O_{NW}(t)$ . Bottom: playing-time  $D_{NW}(t)$ . All calculations are based on RTCP RR for EDGE

The starting rate is configured to be 90 kbps but the transcoder quickly increases it because the network buffer is empty.” Then: ” The gradual rate decrease in the start of the session is caused by the network resource allocation



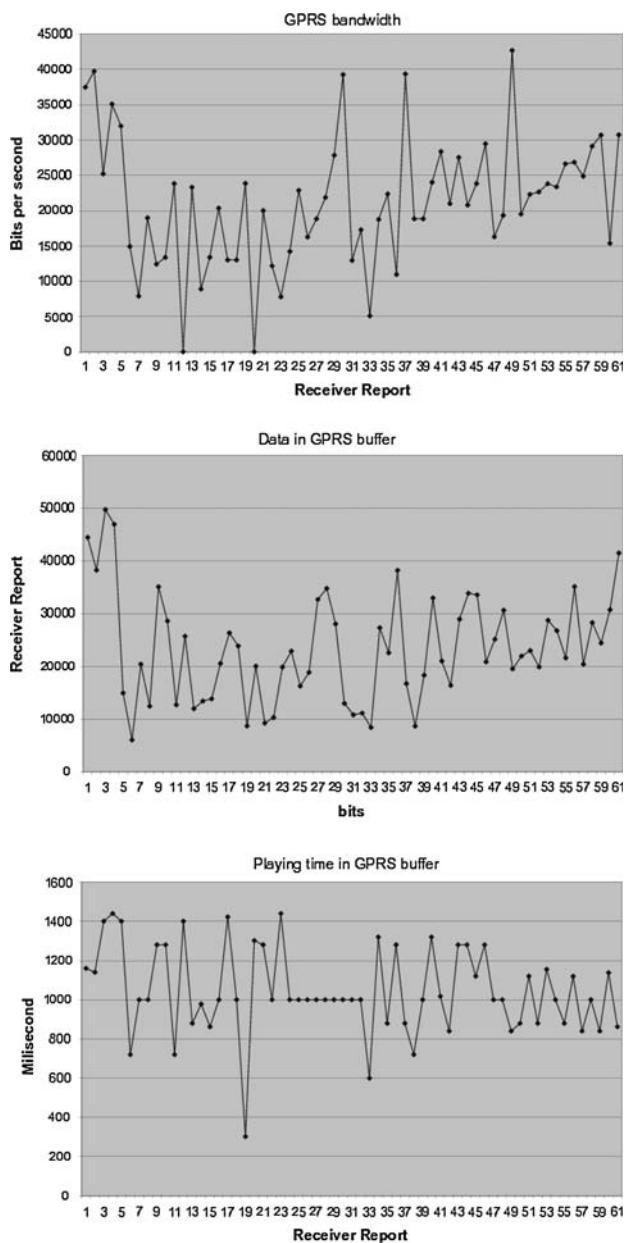


**Fig. 11** Top: Network rate  $R_{NW}(t)$ . Middle: Data level  $O_{NW}(t)$ . Bottom: playing-time  $D_{NW}(t)$ . All calculations are based on RTCP RR for GPRS

mechanism, which allocates more resources only after sensing a demand from the session. The same mechanism caused buffer overflow and packets loss in a constant 280 kbps streaming (Fig. 12). One can see that even when the network decreases its rate relatively slow ASA adapts itself and prevents buffer overflow

Figure 9 (middle) depicts the occupancy level of the network buffer as calculated from the client RTCP RR. We see that the network buffer satisfies the BOC (see Sect. 3.2). It is almost never empty, therefore, the network utilizes its available bandwidth and it is never full

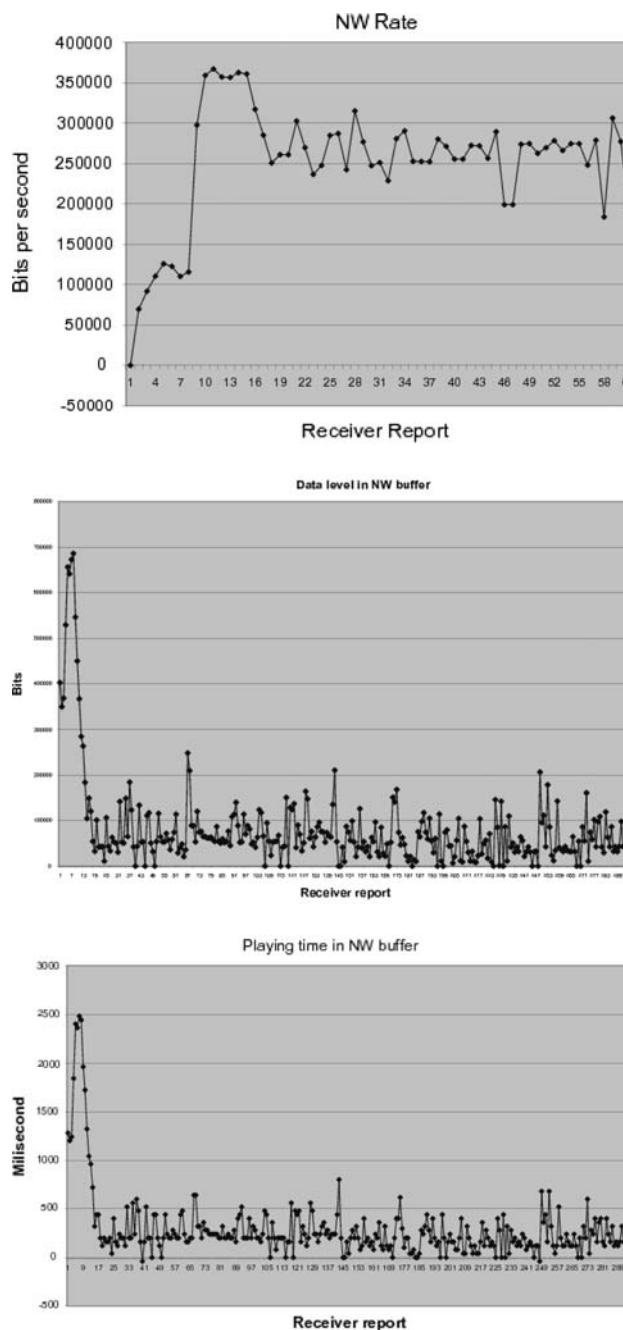


**Fig. 12** Constant rate streaming (without ASA). Top: Network rate  $R_{NW}(t)$ . Middle: Data level  $O_{NW}(t)$ . Bottom: playing-time  $D_{NW}(t)$ . All calculations are based on RTCP RR for UMTS

(700,000 bits) preventing congestion and packet loss. From comparing between the network rate (top) and the data level (middle) in Fig. 9, we see that each time the network rate decreases the network buffer occupancy level increases. The real time transcoder reacts by decreasing the streaming rate to avoid buffer overflow. Figure 9 (bottom) depicts the duration of playing time in the network buffer as calculated from the client RTCP RR. As mentioned before (Sect. 3.3.3), the client stops for re-buffering when

the playing time duration in its buffer reaches 0. The sum of playing time in the client and network buffers is constant; therefore, more playing time in the network buffer means less playing time in the client buffer. The longest playing time recorded in the network buffer during the test session was 940 ms. It means that up to 940 ms were reduced from the cellular client buffer. The initial buffering time in cellular clients is usually 3–5 s; therefore, during the test session there was always enough time in the cellular client buffer to play continuously.

Figures 10 and 11 depict the network rate, the network buffer data and playing time levels during a test session on EDGE and GPRS, respectively. The initial bit rates were 30 kbps for GPRS and 65 kbps for EDGE. We can see that the BOC was always satisfied: the network was fully utilized without causing buffer overflow and packet loss.

Figure 12 depicts streaming without using any rate control. The streaming rate is constantly 280 kbps. At the first 10 s of the session the network rate is low ( $R_{NW}(t) \approx 200$  kbps). However, the streaming server that does not use rate control, continues to send  $R_S(t) = 280$  kbps. The extra bits are accumulated in the network buffer and reach the maximal level of 700,000 bits, which is the maximal size of the network buffer. Thus, remaining bits are discarded. In the first 11 s, 105 from 284 packets were lost which results in an un-usable video. We see that the network buffer playing time reached 2,500 ms. Therefore, the client buffer is missing 2,500 ms. The initial buffering time is 3,000 ms and the client buffer did not stop for re-buffering. This happens because the network buffer was filled before the client buffer emptied and we see packet loss instead of client re-buffering.

## 5.2 Simulation results

The streaming sever, network and client model as was described in Sect. 3.1, was implemented in Matlab. We use ASA to set the streaming server streaming rate. The network rate is determined according to Poisson distribution with average rate  $\lambda$  (see Eq. 3). The simulation parameters are given in Table 1.

**Table 1** Simulation parameters

Parameter	Value
RR period	1 s
Initial buffering	3 s
Initial streaming rate	70 kbps
FPS	15
Frames per packet	1

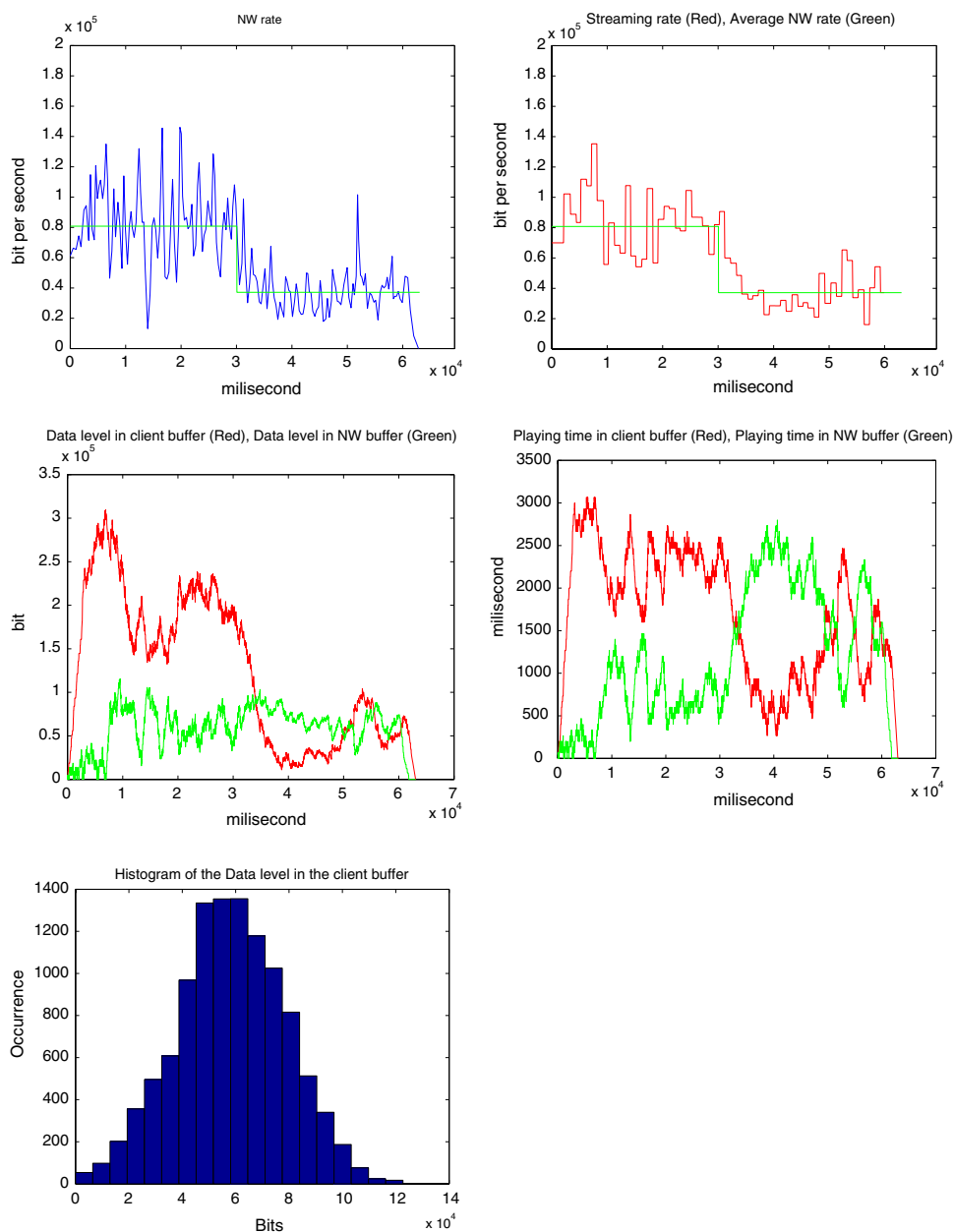
Figure 13 depicts the ASA simulation results. At the top right we see the average available rate and the actual streaming/encoding rate. During the first 30 s, the available network rate is 80,000 bps and during the next 30 s 40,000 bps. At the top left we see the network rate  $R_{NW}(t)$  which follows the available network rate even when it drops in half (at 30 s). The streaming server response is influenced also by the network and client buffers occupancy levels in data size and playing time. At the middle left we see the data level in the NW buffer  $O_{NW}(t)$  and client buffer. The BOC is almost always satisfied in the network buffer because it is almost never empty and never full. Therefore, the calculated usage percentage of the network is 99%. The network buffer data level is constantly around  $DO_{NW} = 60,000$  bits and the maximal data level reached 120,000 bits. We can also see the data level in the client buffer (in red which means that there is always data in the player buffer to continuously play the video and it never reaches high levels to cause buffer overflow. The histogram of the data level  $O_{NW}(t)$  in the NW buffer is given in the bottom left. We see that it resembles a Gaussian around  $DO_{NW} = 60,000$  bits as predicted in the analysis (Sect. 4). At the middle right we see the playing-time in the NW buffer  $D_{NW}(t)$  and client buffer  $D_C(t)$ . The BOC is always satisfied. Therefore, the client never stopped for re-buffering.

Figure 14 depicts streaming without rate control at a constant rate  $R_S(t) = 60,000$  bps. At the top right we see the average available rate and the actual streaming/encoding rate. During the first 30 s the available network rate is 80,000 bps and during the next 30 s 40,000 bps. At the top left we see the network rate  $R_{NW}(t)$ . During the first 30 s, the average available rate is 80,000 bps but the network used only 60,000 bps because this is the rate the streaming server used. (see top right: streaming rate  $R_S(t)$ ). During the next 30 s, the average network rate is 40,000 bps. However, the streaming server that does not use rate control, continues to send  $R_S(t) = 60,000$  bps. The extra bits accumulate in the network buffer (bottom left). During the first 30 s, the network buffer is mostly empty and the network rate is under-used. During the next 30 s, the network buffer is filling, and in real network will overflow. At the bottom right we see the playing-time in the NW buffer  $D_{NW}(t)$  and client buffer  $D_C(t)$ . During the last 30 s, the playing-time in the client buffer  $D_C(t) = 0$ . Therefore, the client does not have media to play and has to stop for re-buffering.

## 6 Conclusion and future work

We introduce in this work the ASA algorithm for adaptive streaming of video over cellular networks. The ASA

**Fig. 13** ASA simulation. *Top left*: Network rate  $R_{NW}(t)$ ; *Top right*: streaming/encoding rate  $R_S(t) = R_S^E(t)$ ; *Middle left*: data level in the NW buffer  $O_{NW}(t)$  and in client buffer; *Middle right*: playing-time in the NW buffer  $D_{NW}(t)$  and in client buffer  $D_C(t)$ ; *Bottom left*: Histogram of the data level in the NW buffer  $O_{NW}(t)$

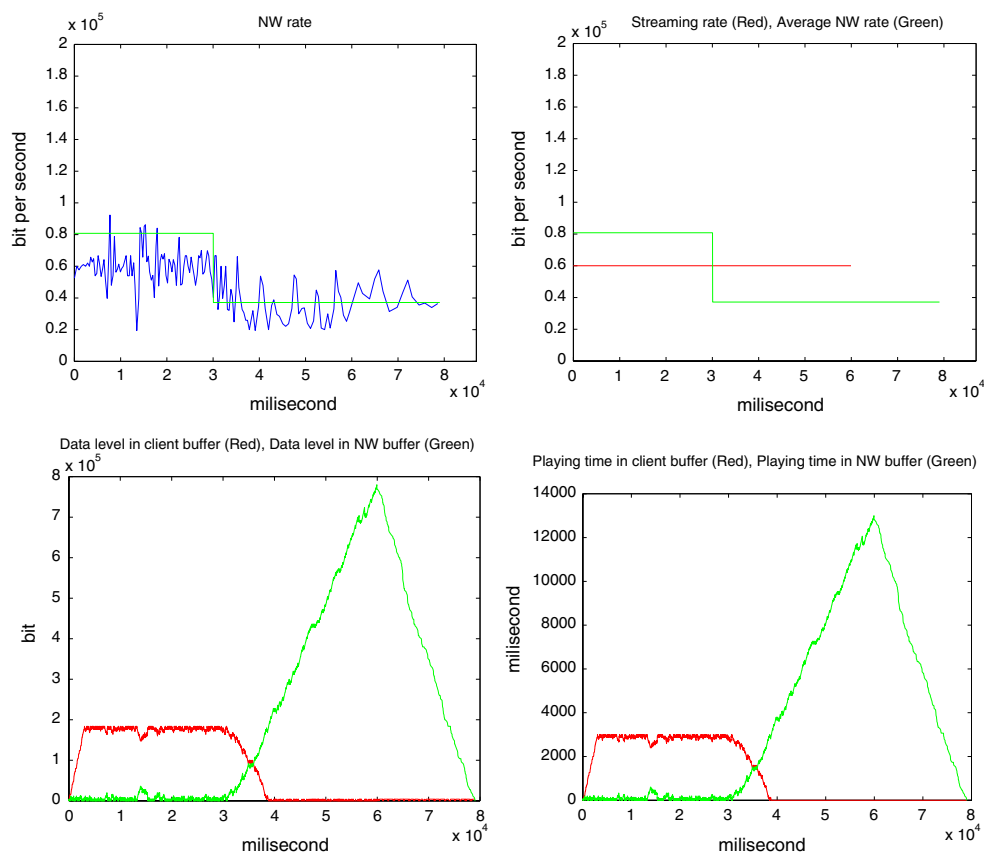


uses the standard RTSP and RTP protocols and can work with any 3GPP standard client. The algorithm satisfies the BOC condition that enables an optimal utilization of the network resources without degrading the video quality. The BOC is satisfied when the streaming-server, network and client buffers stay in a partially full state, never empty and never full, thus, enabling a pause-less streaming without causing congestion and packet loss. The ASA supports separation between the streaming rate and the encoding rate, enabling a better utilization of the network resources. It also enables features like scalable video (a limited number of encoding rates) and fast start (reducing the initial client buffering time by

compromising the initial quality). We tested the ASA on UMTS, EDGE and GPRS networks and found out that the BOC was almost always satisfied.

The ASA can generate a more steady encoding rate by filtering the data from the RTCP receiver reports and by putting some limitation on the streaming and encoding rate change. Furthermore, an automatic configuration of the ASA parameters (current and future) for a given network can simplify its use. Another topic for future work is improving the friendliness of the ASA to TCP streams. Some state-of-the-art algorithms like TFRC pay attention to this issue. It seems that currently most of the video streaming users in the mobile networks do not combine

**Fig. 14** Simulation of constant streaming rate. *Top left:* Network rate  $R_{NW}(t)$ ; *Top right:* streaming/encoding rate  $R_S(t) = R_S^E(t)$ ; *Bottom left:* data level in the NW buffer  $O_{NW}(t)$  and client buffer; *Bottom right:* playing-time in the NW buffer  $D_{NW}(t)$  and client buffer  $D_C(t)$



TCP and UDP streams. Moreover, most of the mobile clients do not allow combining streams unless the mobile client is used as a modem for a computer.

## References

- 3GPP, TSGS-SA, Transparent end-to-end Packet Switched Streaming Service (PSS). Protocols and codecs (Release 6), TS 26.234, v. 6.3.0, 03-2005.
- 3GPP, TSG-SA, Transparent end-to-end Packet Switched Streaming Service (PSS). RTP usage model (Release 6), TR 26.937, v. 6.0.0, 03-2004.
- Kleinrock, L. (1976). *Queueing systems Volume 2: Computer applications*. John Wiley & Sons, Inc.
- IETF, RTP: A Transport Protocol for Real-Time Applications, RFC 3550, July 2003.
- Curcio, I. D. D., & Leon, D. (2005). Application rate adaptation for mobile streaming. *IEEE Int. Symp. on a World of Wireless, Mobile and Multimedia Networks (WoWMoM '05)*, Taormina/Giardini-Naxos (Italy), 13–16, June 2005.
- Curcio, I. D. D., & Leon, D. (2005). Evolution of 3GPP streaming for improving QoS over mobile networks. *IEEE International Conference on Image Processing*. Genova, Italy, 2005.
- Schierl, T., Wiegand, T., & Kampmann, M. (2005). 3GPP compliant adaptive wireless video streaming using H.264/AVC, ICIP 2005. *IEEE International Conference on Image Processing*, Vol. 3, no. 11–14, pp. III-696–III-699, Sept. 2005.
- Floyd, S., Handley, M., Padhye, J., & Widmer, J. (2000). Equation-based congestion control for unicast applications. In *Proceedings of the ACM SIGCOMM 2000*, pp. 43–56, August 2000.
- Floyd, S., & Fall, K. (1999). Promoting the use of end-to-end congestion control in the internet. *IEEE/ACM Transactions on Networking*, 7(4), 458–472.
- Chen, M., & Zachor, A. (2004). Rate control for streaming video over wireless. In *Proceedings of the IEEE INFOCOM*, Hong Kong, China, pp. 1181–1190, 2004.
- Alexiou, A., Antonellis, D., & Bouras, C. (2007). Adaptive and reliable video transmission over UMTS for enhanced performance. *International Journal of Communication Systems*, 20(12), 1315–1335.
- Koenen, R. (2002). MPEG-4 Overview—V.21—Jeju Version, ISO/IEC JTC1/SC29/WG11 N4668, March 2002.
- Farber, N., & Girod, B. (1997). Robust H.263 compatible video transmission for mobile access to video servers. In *Proc. IEEE International Conference on Image Processing (ICIP-97)*, Santa Barbara, CA, USA, Vol. 2, pp. 73–76, October 1997.
- Joint Video Team of ITU-T and ISO/IEC JTC 1, Draft ITU-T Recommendation and Final Draft International Standard of Joint Video Specification (ITU-T Rec. H.264—ISO/IEC 14496-10 AVC), document JVT-G050r1, May 2003; technical corrigendum 1 documents JVT-K050r1 (non-integrated form) and JVT-K051r1 (integrated form), March 2004; and Fidelity Range Extensions documents JVT-L047 (non-integrated form) and JVT-L050 (integrated form), July 2004.
- Schierl, T., Kampmann, M., & Wiegand, T. (2005). H.264/AVC interleaving for 3G wireless video streaming, ICME 2005. *IEEE International Conference on Multimedia and Expo*, no. 4, pp. 6–8, July 2005.



16. Skellam, J. G. (1946). The frequency distribution of the difference between two Poisson variates belonging to different populations. *Journal of the Royal Statistical Society: Series A*, 109(3), 296.
17. IETF, Real Time Streaming Protocol (RTSP), RFC 2326, April 1998.

### Author Biographies



**Y. Falik** is the CTO of RTC Ltd. which specializes in Image/Video processing and computer vision. He specializes in video/image compression and video streaming. Prior to RTC he managed algorithms groups in Adamind (2005–2007) and Emblaze (2000–2005). Previously, he developed innovative PowerPC chip that runs on compressed code in Motorola (1997–2000), and worked for a scientific group in the Israeli army (1993–1996). He holds an

M.Sc in computer science from the Tel-Aviv University.



**A. Averbuch** was born in Tel Aviv, Israel. He received the B.Sc and M.Sc degrees in Mathematics from the Hebrew University in Jerusalem, Israel in 1971 and 1975, respectively. He received the Ph.D degree in Computer Science from Columbia University, New York, in 1983. During 1966–1970 and 1973–1976 he served in the Israeli Defense Forces. In 1976–1986 he was a Research Staff Member at IBM T.J. Watson Research Center, York-

town Heights, in NY, Department of Computer Science. In 1987, he joined the School of Computer Science, Tel Aviv University, where

he is now Professor of Computer Science. His research interests include applied harmonic analysis, wavelets, signal/image processing, numerical computation and scientific computing (fast algorithms).



**U. Yechiali** is professor emeritus from the operations research and statistics in the Department of Statistics and Operations Research (chair the department twice), School of Mathematical Sciences, Tel Aviv University, Israel. His major research fields are: Queueing theory and its applications, performance evaluation, telecommunications, reliability, operations research modeling, applied probability. He got his B.Sc. (cum laude) in Industrial and Management

Engineering, Technion, Haifa, Israel in 1964, M.Sc. in Operations Research, Technion, Haifa, Israel in 1966 and his Dr. Eng. Sci. in Operations Research, Columbia University, New York, USA in 1969. He had visiting professorship in New York University, Columbia university. He got in 2004 the ORSIS Award for “Life Achievement” in Operations Research. He was an Associate Editor, Probability in the Engineering & Informational Sciences, Member of Editorial Board, European Journal of Operational Research and Board of Editors, Advances in Performance Analysis.